ACS APPLIED MATERIALS & INTERFACES

Research Article

www.acsami.org

Three-Dimensional Conductive Nanocomposites Based on Multiwalled Carbon Nanotube Networks and PEDOT:PSS as a Flexible Transparent Electrode for Optoelectronics

Er-Chieh Cho,[†] Chiu-Ping Li,[‡] Jui-Hsiung Huang,[‡] Kuen-Chan Lee,*[,§] and Jen-Hsien Huang*[,‡]

[†]Department of Clinical Pharmacy, School of Pharmacy, College of Pharmacy, Taipei Medical University, Taipei, Taiwan

[‡]Department of Green Material Technology, Green Technology Research Institute, Chinese Petroleum Corporation (CPC Corporation), Kaohsiung, Taiwan

[§]Department of Fragrance and Cosmetic Science, Kaohsiung Medical University, Kaohsiung, Taiwan

ABSTRACT: We have synthesized conductive nanocomposites composed of multiwalled carbon nanotubes (MWCNTs) and Au nanoparticles (NPs). The Au NPs with an average size of approximately 4.3 nm are uniformly anchored on the MWCNT. After being exposed to microwave (MW) plasma irradiation, the anchored Au NPs melt and fuse, leading to larger aggregates (34 nm) that can connect the MWCNT forming a three-dimensional conducting network. The formation of a continuous MWCNT network can produce more a conductive pathway, leading to lower sheet resistance. When the Au-MWCNT is dispersed in the highly conductive polymer, poly(ethylene dioxythiophene):polystyrenesulfonate (PEDOT:PSS), we can obtain solution-processable composite formulations for the preparation of a flexible transparent electrode. The resulting Au-MWCNT/PEDOT:PSS hybrid films possess a sheet resistance of 51 Ω/sq with a transmittance of 86.2% at 550 nm. We also fabricate flexible organic solar cells and electrochromic devices to demonstrate the potential use of the as-prepared composite electrodes. Compared with the indium tin oxide-based devices, both the solar cells and electrochromic devices with the composites incorporated as a transparent electrode deliver comparable performance.

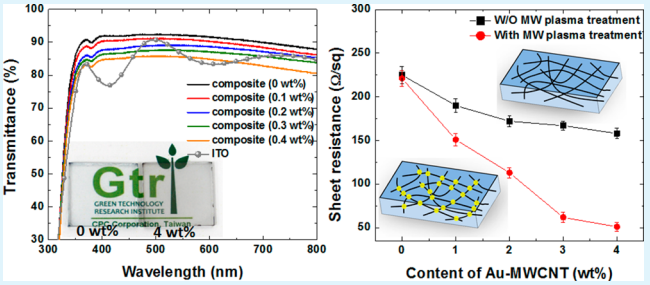

KEYWORDS: *multiwalled carbon nanotube, Au nanoparticles, microwave plasma irradiation, solar cells, electrochromic devices*

1. INTRODUCTION

Recently, flexible organic optoelectronics have attracted a great deal of attention because of their lightness, thinness, and excellent mechanical flexibility.[1−3] The transparent electrode for flexible optoelectronics should satisfy special requirements, such as being bendable, having solvent resistance, and being highly conductive and transparent. Currently, indium tin oxide (ITO) films are most commonly used for the transparent electrode. However, it has many drawbacks, including its high price, complicated process requirements, sensitivity toward acid environments, and poor adhesion with organic and polymeric materials. It has been reported that approximately 37−50% of the material cost for polymer solar cells is from ITO.[4] Therefore, ITO cannot be used as the transparent electrode for next-generation optoelectronic devices.

As one of the most successful conducting polymers, PEDOT:PSS has attracted a great deal of interest over the past two decades.[5−8] Its high conductivity and transparency, low sheet resistance, and versatility of processing from an aqueous solution make it an attractive choice for the transparent electrode for organic optoelectronics. Recently, a couple of investigations have been reported the enhancement of the conductivity of PEDOT:PSS. Kim et al. found the conductivity of PEDOT:PSS can be enhanced by ∼2 orders in magnitude via addition of dimethyl sulfoxide (DMSO) or dimethylformamide (DMF).[9] Other organic compounds such as ethylene glycol,[10] polyalcohols,[11−17] an anionic surfactant,[18,19] and an organic acid[20−22] were also investigated for the conductivity enhancement of PEDOT:PSS. It has been concluded that these additives can enhance the phase separation between the conductive PEDOT and the insulating PSS domains, leading to a more PEDOT conductive pathway.

In particular, composites of carbon-based materials and PEDOT:PSS have attracted a great deal of attention because of the potential creation of synergistic effects on the thermal and electrical properties. To further improve the conductivity and reduce the sheet resistance of PEDOT:PSS, many researchers have studied carbon nanotube (CNT)/PEDOT composite films.[23−25] The conductivity of the CNT/PEDOT composites is determined significantly by the formation of a CNT conducting pathway that depends on the CNT concentration and dispersibility within the polymer matrix. However, the

Received: April 13, 2015
Accepted: May 13, 2015
Published: May 13, 2015

DOI: 10.1021/acsami.5b03159
ACS Appl. Mater. Interfaces 2015, 7, 11668−11676

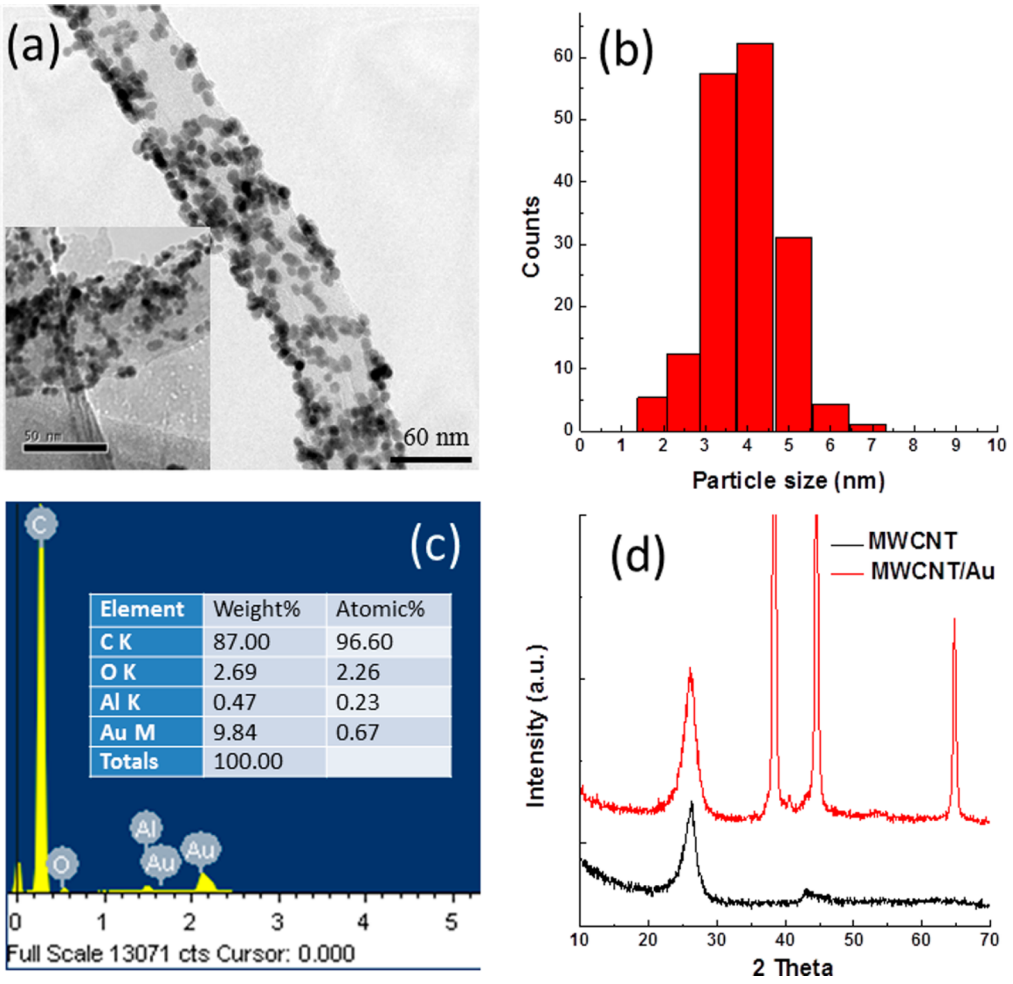

Figure 1. Synthesis of Au-MWCNT composites. (a) Representative TEM image of Au NPs attached to MWCNTs. (b) Histograms of the size distribution of Au NPs. (c) EDX pattern of as-produced Au-MWCNT composites, indicating the atomic percentage of Au. (d) XRD pattern of the pristine MWCNT and Au-MWCNT composites.

higher CNT concentration would dramatically decrease the transmittance. Moreover, the common surfactants used for dispersing the carbon-based materials are nonconductive. These surfactants also impede the formation of the PEDOT and CNT continuous pathway.

To overcome these problems, in this work, we demonstrated the preparation of Au NPs supported on MWCNTs by using a simple polyol process with surfactant-assisted sonication. Via probe sonication treatment, the Au-MWCNT composites can be uniformly dispersed with PEDOT:PSS without precipitation. The produced homogeneous Au-MWCNT/PEDOT:PSS composite solution can form a uniform film with a smooth surface via a spin-coating method. To create a more MWCNT conducting pathway within the PEDOT:PSS matrix, we treat the composites with MW plasma irradiation, which can provide rapid heating and a uniform temperature for fusing and coalescing the Au NPs into large Au NPs. The coalesced Au NPs can act as conducting bridges to connect the MWCNTs, leading to more intra- and interjunctions between the MWCNTs. The resulting composite films exhibit improved optoelectronic properties, and they possess a sheet resistance of 51 Ω/sq with a transmittance of 86.2% at 550 nm. Finally, we also fabricated organic solar cells and electrochromic devices to demonstrate the potential use of composite electrodes.

2. EXPERIMENTAL SECTION

2.1. Preparation of Au-MWCNT Composites. Initially, 100 mg of MWCNT and 300 mg of sodium dodecyl sulfate were mixed with 100 mg of deionized water in a 500 mL flask to produce a homogeneous solution using probe-type sonication (Sonics VCX750, supplied by Sonics & Materials, Inc.). For the polyol process, the as-prepared Au organosol, containing 43.4 mg of $HAuCl_4$ dissolved in 100 mL of ethylene glycol, was added dropwise to the MWCNT dispersed solution described above under a nitrogen atmosphere. Subsequently, the mixture was stirred and heated to 105 °C at a heating rate of 2 °C/min, and it was kept at 105 °C for 2 h. Finally, the Au-MWCNT composites were collected by filtration; they were then washed with copious amounts of ethyl alcohol and dried in vacuum at 80 °C for 8 h. MW plasma irradiation was performed by a system that consisted of a MW oven with two drilled holes on the upper part and a quartz chamber made of Pyrex, which was connected to an argon cylinder. The air pressure was controlled in the range of 0.1−2.0 Torr, and the operation time was fixed at 3 min.

2.2. Preparation of a Au-MWCNT/PEDOT:PSS Solution. The modified PEDOT:PSS (Clevios PH1000) was prepared by adding DMSO (5 vol %) to the as-bought PEDOT:PSS. The modified PEDOT:PSS was filtered (0.45 μm, PVDF) at room temperature. Subsequently, different amounts of Au-MWCNT composites (0−0.4 wt %) were added to the PEDOT:PSS solution. With probe-type sonication, the Au-MWCNT can be dispersed in the PEDOT:PSS uniformly without precipitation. For the dispersed process, different sonication powers and times were used at 20 °C (20% and 30 s, 30%

DOI: 10.1021/acsami.5b03159
ACS Appl. Mater. Interfaces 2015, 7, 11668−11676

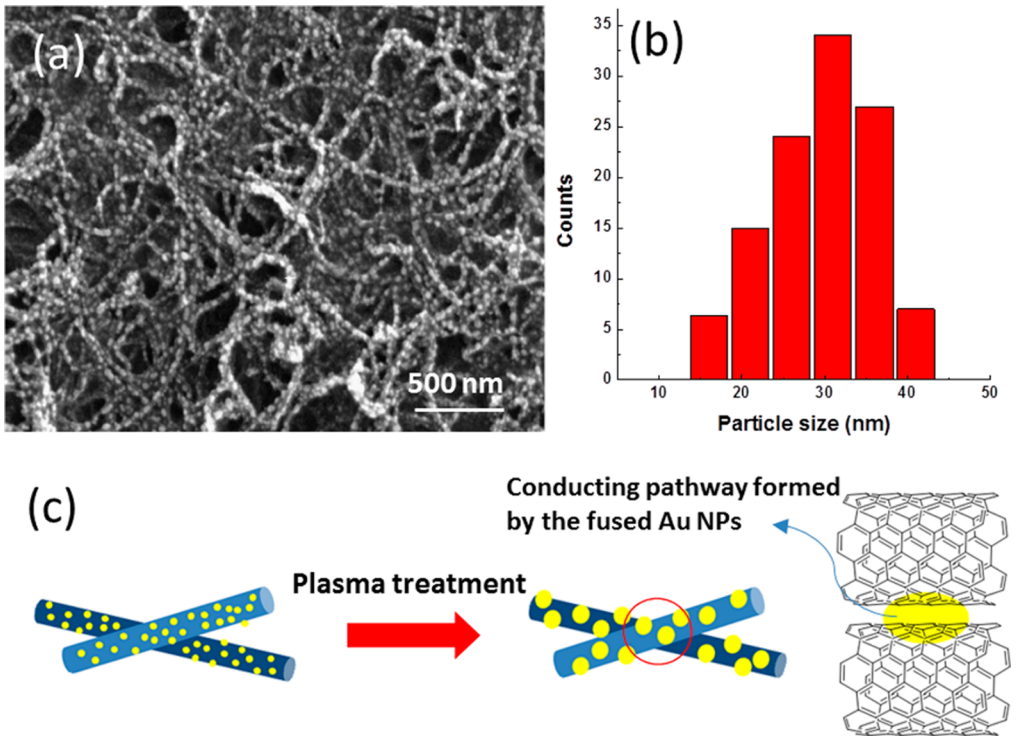

Figure 2. (a) SEM image of the representative Au-MWCNT composites after MW plasma treatment. (b) Corresponding particle size distribution of Au NPs. (c) Schematic illustration of the Au NPs attached to MWCNTs after MW plasma irradiation.

and 2.5 min, 40% and 15 min, 30% and 2.5 min, and 40% and 5 min, respectively).

2.3. Characterization. A JEOL 2010 transmission electron microscope (TEM) was used to examine the morphology of the Au-MWCNT composites. Elemental analysis was performed with an energy-dispersive X-ray spectroscopy (EDX) system coupled to the TEM. The transmittance spectra of the carbon composite films were recorded using a Jasco-V-670 UV–vis spectrophotometer. The surface morphologies of the carbon composite films were investigated using atomic force microscopy (AFM) (Digital Instrument NS 3a controller equipped with a D3100 stage) and scanning electron microscopy (SEM) (Hitachi S-4700). The sheet resistance of the composites was measured using the four-point probe with a Keithley 2400 sourcemeter current source. The work function of the electrode was measured by X-ray photoelectron spectrometry (XPS/UPS) using a PHI 5000 VersaProbe (ULVAC-PHI, Chigasaki, Japan) system with He(I) ($h\nu$ = 21.2 eV) as the energy source. Spectroelectrochemical data were recorded using a Shimadzu UV-1601PC spectrophotometer.

2.4. Fabrication and Characterization of Organic Solar Cells. The polymer solar cells consisted of a layer of the poly(3-hexylthiophene):[6,6]-phenyl-C61-butyric acid methyl ester (P3HT:PCBM) blend thin film sandwiched between the Au-MWCNT/PEDOT:PSS electrode and a metal cathode. Precleaned glass substrates were treated with O_2 plasma to activate the surface. Typically, the Au-MWCNT/PEDOT:PSS electrode was spin-coated at 2000 rpm for 60 s. The electrodes were then annealed on a hot plate at 110 °C for 20 min. Subsequently, the active layer [P3HT:PCBM, 1:1 (w/w); 2% in dichlorobenzene] was then spin-coated by the slow-growth method.[26] Finally, thermal evaporation of Al and Ca provided the reflective cathodes. Solar cell testing was performed inside a glovebox under simulated AM 1.5G irradiation (100 W/cm^2) using a Xe lamp-based solar simulator (Thermal Oriel 1000W). The light source was a 450 W Xe lamp (Oriel Instrument, model 6266) equipped with a water-based IR filter (Oriel Instrument, model 6123NS). The light output from the monochromator (Oriel Instrument, model 74100) was focused onto the tested solar cell. Electrical characteristics were measured at room temperature under a N_2 atmosphere using an HP 4156C apparatus placed within a glovebox.

3. RESULTS AND DISCUSSION

The TEM was used to monitor the morphology of the Au-MWCNT as shown in Figure 1a. Morphological observation illustrates the Au NPs are uniformly attached to MWCNTs and after the modification still preserved the structure of MWCNTs. The anchored Au NPs have spherical shapes and narrow size ranges. It is worth mentioning that many Au NPs were formed in the cross-linked Au-MWCNT composites. It is believed that these Au NPs can enhance the intrajunctions between the Au-MWCNT composites, resulting in improved conductivity. As shown in Figure 1b, the particle sizes of Au NPs ranged between 1.8 and 6.9 nm and their average size is around 4.3 nm. Furthermore, the elementary composition of the Au-MWCNT composites is confirmed by EDX analysis (Figure 1c). The result shows that the chemical composition of the Au-MWCNT is 9.84 wt % Au. The XRD measurement was also performed to further confirm the formation of Au NPs. As shown in Figure 1d, two peaks located at 38° and 44° can be found for the Au-MWCNT composites, which correspond to the (111) and (200) crystal planes, respectively. No characteristic peaks of other impurities are found. This result suggests the Au NPs are uniformly distributed on the MWCT surface.

To improve the electrical and mechanical properties of Au-MWCNT composites by enhancing the connection between the MWCNTs, in this study, we annealed the Au NPs under MW plasma irradiation. Panels a and b of Figure 2 show the SEM image and the histograms of the representative Au-MWCNT composites after plasma treatment, respectively. Compared with the sample without plasma annealing, it can be seen the Au NPs attached to the MWCNT (34 nm) are larger than that of the as-prepared NPs (4.3 nm). During plasma

DOI: 10.1021/acsami.5b03159
ACS Appl. Mater. Interfaces 2015, 7, 11668–11676

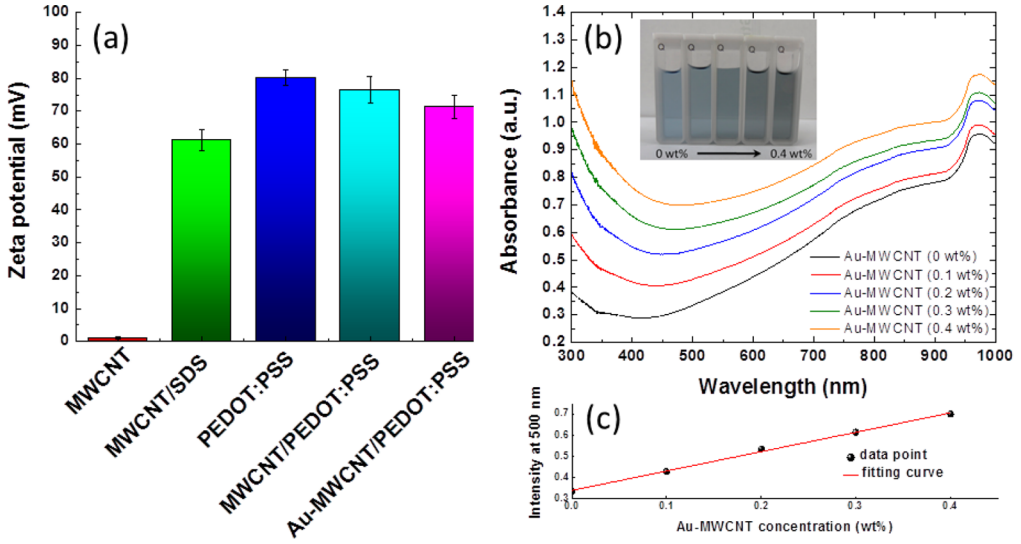

Figure 3. Preparation of a Au-MWCNT/PEDOT:PSS suspension. (a) ζ potential of MWCNT in different solutions. (b) Absorption of the Au-MWCNT/PEDOT:PSS with various Au-MWCNT concentrations. The composite solutions were diluted with water [1:20 (v/v) Au-MWCNT/PEDOT:PSS:water]. The inset shows the images of the diluted composite solutions. (c) Plot of absorption intensity vs Au-MWCNT concentration.

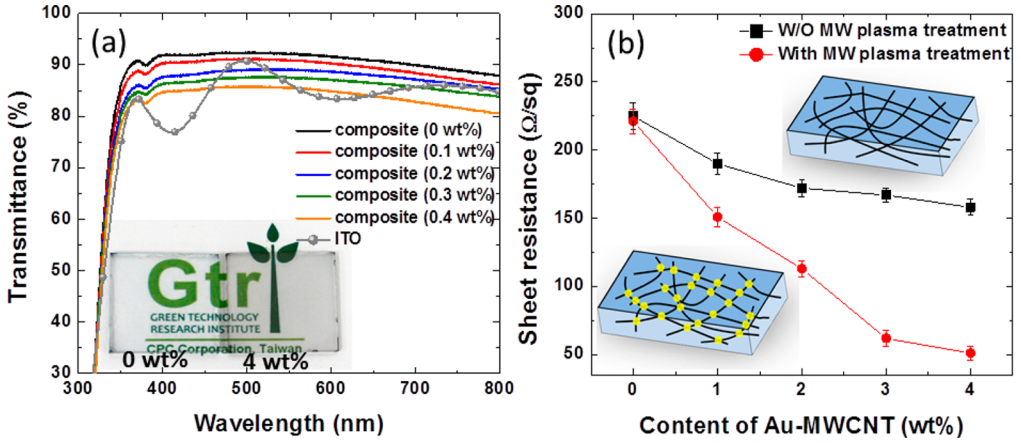

Figure 4. Transmittances and resistances of the carbon composite films. (a) Transmission spectra of Au-MWCNT/PEDOT:PSS films featuring different Au-MWCNT contents. (b) Effect of MW plasma and loading amount of Au-MWCNT on sheet resistance of the composite films. Plasma irradiation can sinter the Au NPs, leading to a better connection between MWCNTs, which provides effective conducting pathways and reduces the sheet resistance.

irradiation, the Au NPs melt and fuse, leading to larger aggregates. As shown in Figure 2c, this coalescent process offers a stronger, more cohesive metallic Au-MWCNT adhesion, where the Au NPs also serve as a junction bridge between the MWCNTs. This facilitates the formation of a three-dimensional composite network that reduces the energy barrier for electron transport. We believe that the plasma treatment can enhance not only the conductivity but also the mechanical strength.

For the application of the transparent electrode, CNT is an attractive candidate because of its high conductivity, stability, and optical transmittance. However, CNT has an intrinsic problem because it is difficult to disperse and use to form a smooth film. The CNT without full dispersion would easily form coarse CNT bundles, leading to an uneven surface morphology.[27] In a transparent electrode, such bundles would be problematic for device fabrication because they might protrude through the active layers and, thereby, result in shortening. Recently, several types of stabilizers have been used to disperse carbon nanotubes such as surfactants,[28−31] polymers,[32,33] and biomaterials.[34,35] Most dispersants are electrical insulators that hinder the transport of electrons across the junctions. In this study, PEDOT:PSS, doped with DMSO, was used to disperse MWCNTs in water. The PEDOT:PSS can act as a surfactant to disperse MWCNT and prevent it from settling and aggregating.[36−38] Moreover, the PEDOT:PSS can also fill the space between the MWCNT network forming a fully continuous, conductive composite film. Figure 3a shows the measured ζ potential of pristine MWCNTs and MWCNTs dispersed with sodium dodecyl sulfate (SDS) and PEDOT:PSS. The ζ potentials of the MWCNT/SDS, PEDOT:PSS, MWCNT/PEDOT:PSS, and Au-MWCNT/PEDOT:PSS were 61.3, 80.1, 76.4, and 71.3 mV, respectively. Such a high ζ potential of the MWCNT/PEDOT:PSS indicates that the MWCNT can be stabilized within the PEDOT:PSS.[39] It should be noted that the PSS content usually is 2.5 times higher than the PEDOT content. Excess PSS has also been reported to be a good dispersant for CNT.[40] The slight decrease in the ζ potential of Au-MWCNT/PEDOT:PSS (71.3 mV) compared with that of MWCNT/PEDOT:PSS (76.4 mV) is due to the higher bulk density contributed from the

DOI: 10.1021/acsami.5b03159
ACS Appl. Mater. Interfaces 2015, 7, 11668−11676

decorated Au NPs. Absorption spectroscopy can be used to further shed light on the dispersibility of the Au-MWCNT/PEDOT:PSS colloidals. The absorption spectra were recorded with a UV−vis spectrometer with wavelengths of 300−1000 nm at different concentrations of Au-MWCNT from 0 to 0.4 wt % as shown in Figure 3b. With increasing Au-MWCNT contents, the absorption of the colloidals increases in the range between 300 and 1000 nm. The images of the Au-MWCNT/PEDOT:PSS with various Au-MWCNT contents are also shown in the inset of Figure 3b. A linear relationship can be seen in Figure 3c and follows the Lambert−Beer law well,[41] suggesting that the Au-MWCNT can form a uniform and stable colloidal after dispersion in the PEDOT:PSS. The MWCNT/PEDOT:PSS can remain highly dispersed without precipitation after centrifugation at 3000 rpm. These results suggest that the PEDOT:PSS can be applied as a conductive surfactant to disperse the MWCNT.

We characterized the optical and electrical properties of the composite films using UV−vis spectroscopy (at normal incidence) and a four-point probe. Figure 4a shows the transmittance spectra of ITO and Au-MWCNT/PEDOT:PSS composites with various MWCNT contents. Even when the content of MWCNT is 0.4 wt %, the transmittance of the composite still can be as high as 80% in the range between 400 and 800 nm. Compared with that of the ITO substrate, the transmittance of the composites is higher in the violet, blue, and green regions. The transmittance values of the composites with 0, 0.1, 0.2, 0.3, and 0.4 wt % Au-MWCNT are 92.1, 90.8, 89.1, 87.3, and 86.2%, respectively, at 550 nm, including the glass substrate. Figure 4b shows the variation of sheet resistance for the composite films with different Au-MWCNT contents. It can be seen that the sheet resistance decreases with an increasing content of Au-MWCNT. Moreover, the sheet resistance for the Au-MWCNT/PEDOT:PSS can be further decreased dramatically after MW plasma treatment. For the composite film with 0.4 wt % Au-MWCNT, the sheet resistance reaches as low as 51 Ω/sq, after plasma irradiation. This value is much lower than that of the sample without treatment (158 Ω/sq). It should be noted that the sheet resistance of pristine PEDOT:PSS remains unchanged even after MW plasma irradiation. This indicates the enhancement of conductivity is completely contributed by the coalescence of the Au NPs induced from the plasma treatment. The larger Au NPs play as a conductive bridge to connect the MWCNTs, thereby producing the three-dimensional MWCNT network within the PEDOT:PSS matrix. As a result, the favorable morphology is effective in increasing the number of charge transfer pathways and minimizing the barrier for charge transfer between the MWCNTs, which in turn reduces the sheet resistance.

We also used AFM to characterize the surface topography of the PEDOT:PSS and Au-MWCNT/PEDOT:PSS (0.4 wt %). The morphology of PEDOT:PSS reveals a smooth surface without any features (Figure 5a) The AFM profile reveals that the root-mean-square (rms) surface roughness of the PEDOT:PSS is approximately 1.13 nm. In contrast, for the hybrid, the morphology exhibits many MWCNTs running across the surface as shown in Figure 5b. It can be seen that the MWCNTs are well-dispersed without aggregation and distributed on the surface uniformly. The rms roughness of the composite only slightly increases from 1.13 to 4.12 nm. Such an even surface, transparency, and high conductivity make the composites alternatives to ITO and other transparent conducting materials.

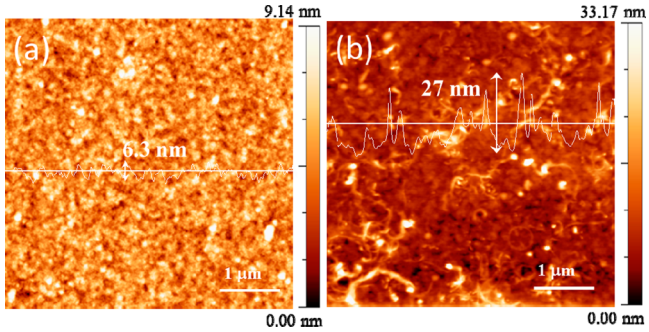

Figure 5. Representative images of the surface morphologies of the carbon-based films. (a) Pristine PEDOT:PSS film. (b) Au-MWCNT/PEDOT:PSS composite film (0.4 wt %).

To investigate the flexibility of the Au-MWCNT/PEDOT:PSS electrodes, we coated the composites on the PET substrate and used the sheet resistance as a parameter to explore the stability of the Au-MWCNT/PEDOT:PSS and ITO/PET under various bending conditions. Figure 6a displays

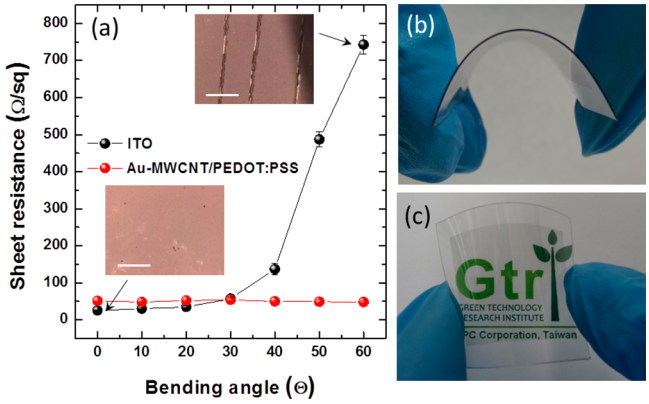

Figure 6. Bending tests of films of ITO and Au-MWCNT/PEDOT:PSS on flexible PET substrates. (a) Sheet resistances of Au-MWCNT/PEDOT:PSS and ITO films on PET substrates, plotted with respect to the bending angle. The inset is the corresponding optical image for the ITO/PEDT before and after bending. (b and c) Representative photographs of a Au-MWCNT/PEDOT:PSS flexible electrode subjected to bending.

the correlation between the bending angle and conductance for the composite and ITO/PET. ITO/PET underwent an irreversible loss of electrical conductivity because of the propagation cracks throughout its crystalline networks. The corresponding optical images are also shown in the inset. Meanwhile, the composite film exhibits comparable sheet resistance before and after bending test cycles by virtue of its high flexibility and mechanical strength. The sheet resistance of the ITO film increased from 24 to 743 Ω/sq after blending at 60°, while Au-MWCNT/PEDOT:PSS reveals similar values (~51 Ω/sq). In light of mechanical measurements, the as-synthesized hybrid composite film evidently possesses a much-enhanced mechanical flexibility versus those of ITO films and is well suited for conductive platforms for flexible electronics. The images of the composite films under bending are also shown in panels b and c of Figure 6.

To improve our understanding of the physical property of the as-prepared composites, we measured the shift in the secondary electron cutoff of the composite films to determine

DOI: 10.1021/acsami.5b03159
ACS Appl. Mater. Interfaces 2015, 7, 11668−11676

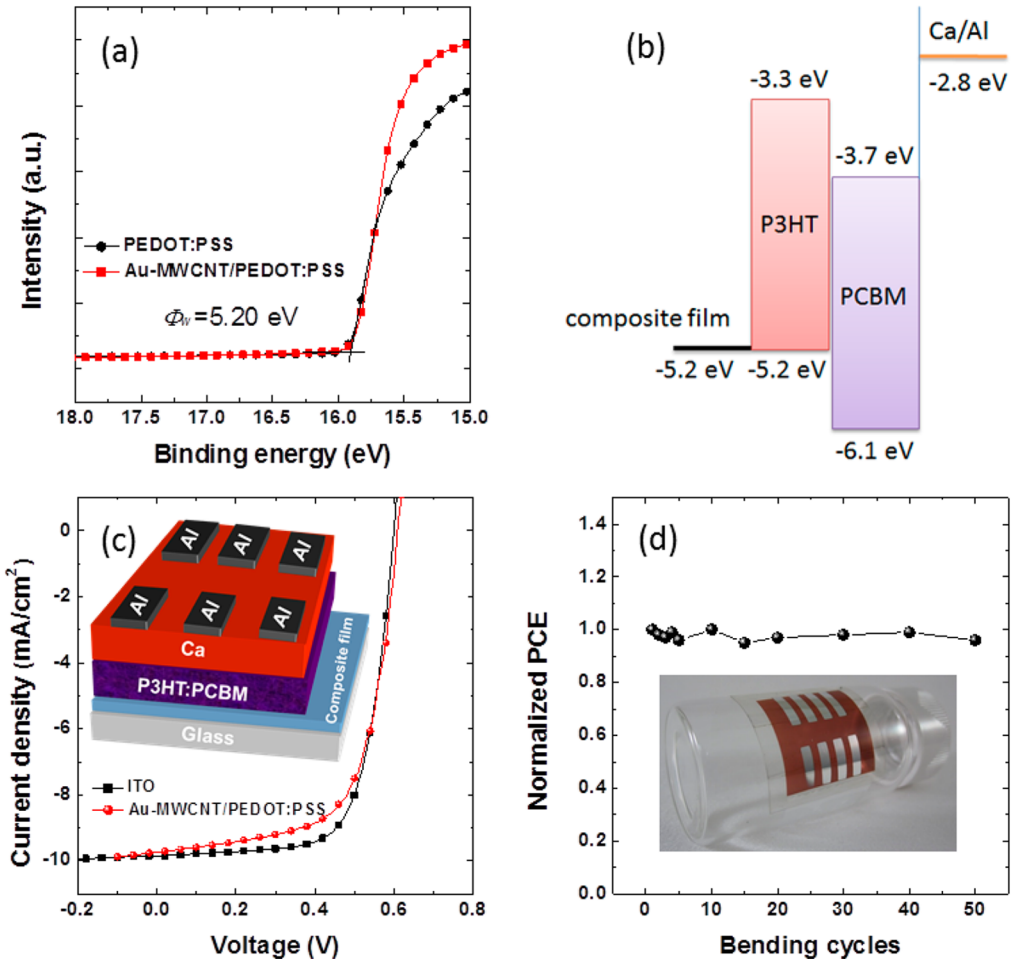

Figure 7. Application of the Au-MWCNT/PEDOT:PSS composite for flexible organic solar cells. (a) Measurement of the value of the work function of the composite film. (b) Energy level diagrams of the P3HT:PCBM solar cell featuring a Au-MWCNT/PEDOT:PSS-based transparent electrode. (c) *J*–*V* characteristics of P3HT:PCBM solar cells. (d) Effect of bending cycle on cell performance. The results indicate that the Au-MWCNT/PEDOT:PSS can be used as a flexible transparent electrode for organic solar cells.

their work function. As shown in Figure 7a, we observe the values of the work function (5.2 eV) for the Au-MWCNT/PEDOT:PSS (0.4 wt %) and pristine PEDOT:PSS are almost the same. The results indicate the composite is suitable for not only transparent electrode but also the hole collection layer for organic solar cells because of its high work function. Therefore, to apply the composite as a transparent electrode in an organic solar cell, P3HT:PCBM-based solar cells were fabricated. The schematic energy levels of Au-MWCNT/PEDOT:PSS together with others materials used in our study are also shown in Figure 7b. Figure 7c presents the current–voltage (*J*–*V*) curves of solar cells. For the purpose of comparison, the devices based on ITO (20 Ω/sq) and Au-MWCNT/PEDOT:PSS (0.3 wt %) as a transparent electrode were both fabricated. The Au-MWCNT/PEDOT:PSS-based device delivered a short-circuit current (J_{SC}) of 9.87 mA/cm^2; with an open-circuit voltage (V_{OC}) of 0.60 V and a fill factor (FF) of 65.3%, the power conversion efficiency (PCE) was 3.85%. This value can rival that of the ITO-based device (4.10%). To investigate the effect of bending on the cell performance, we also fabricated the organic solar cells on the PET substrate with the composites as an electrode. As shown in Figure 7d, the performance was evaluated up to 50 bending cycles, and the PCE values of the device remained almost unchanged. The negligible variation in cell performance indicates that the Au-MWCNT/PEDOT:PSS is flexible and does not suffer from severe cracks or defect formation under the bending conditions.

The adhesion between the conductive layer and substrate is also an important issue for the transparent electrode to be used in aqueous media, especially in an electrochemical system. In this study, we also evaluated the feasibility of applying the composite as a transparent electrode for the electrochromic device. Figure 8a presents the optoelectrochemical spectral series for the PEDOT electrochemically deposited on the Au-MWCNT/PEDOT:PSS (0.3 wt %). It can be seen that the PEDOT can be successfully stepped between 1.0 and −1.0 V on the conductive composites. Figure 8b displays the switching of the PEDOT between 1.0 and −1.0 V at an interval of 10 s in 0.1 M $LiClO_4$/acetonitrile. We observed a contrast ($\Delta\%T$) of 52.8% at 600 nm for PEDOT deposited on the composite film, which is slightly larger than the sample (49.3%) on the ITO electrode. The slightly higher contrast resulted from the better transparency of the Au-MWCNT/PEDOT:PSS at 600 nm (Figure 4a). The coloration efficiency is the most important parameter for electrochromic materials. Here, we also study the effect of the transparent electrode on the coloration efficiency (CE). The changes in optical density (ΔOD) as a function of charge ingress or egress are shown in Figure 8c at a monochromatic wavelength of 600 nm. Via calculation of the slope of the plot of ΔOD versus charge, the CE of PEDOT can

DOI: 10.1021/acsami.5b03159
ACS Appl. Mater. Interfaces 2015, 7, 11668–11676

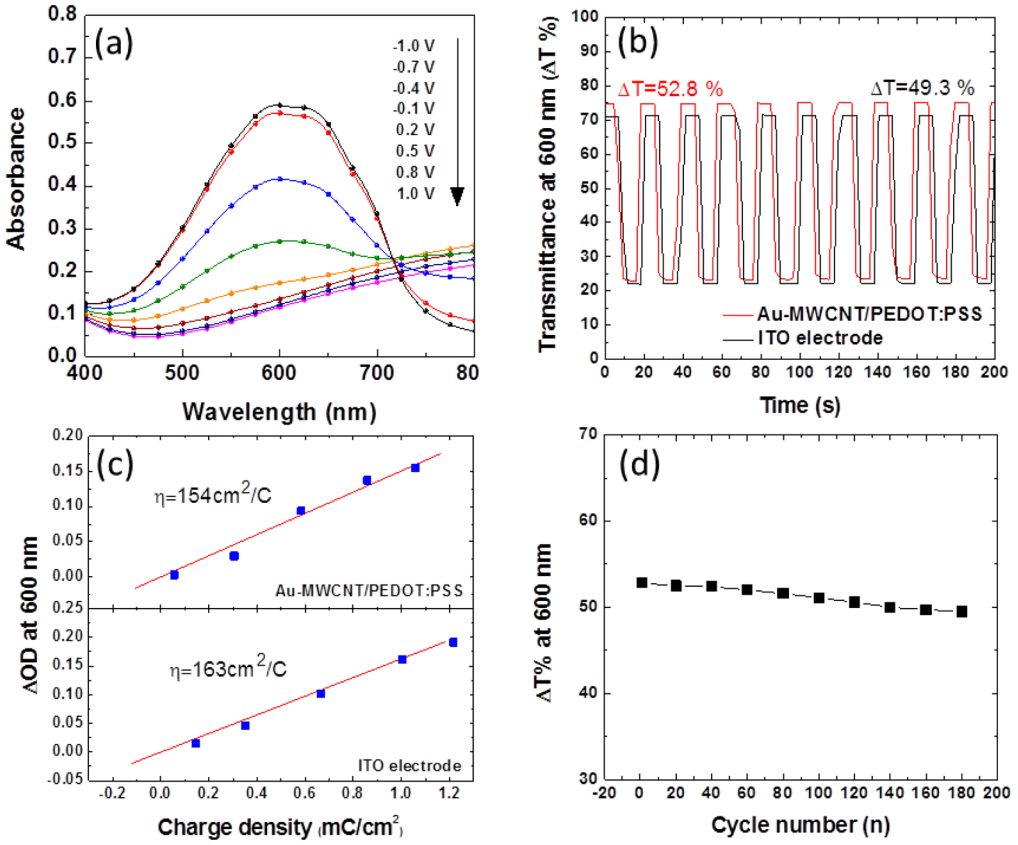

Figure 8. Application of the Au-MWCNT/PEDOT:PSS composite for electrochromism. (a) *In situ* UV−vis absorption of PEDOT films at various potentials in 0.1 M $LiClO_4$/acetonitrile. (b) *In situ* transmittance response of the PEDOT during repeat potential steps switched between −1.0 and 1.0 V [vs Ag/Ag^+(acetonitrile)]. (c) Optical density changes of PEDOT thin films as a function of intercalated charge density. (d) Long-term stability of PEDOT on the Au-MWCNT/PEDOT:PSS electrode.

be determined. As shown in Figure 8c, the calculated CEs of PEDOT deposited on Au-MWCNT/PEDOT:PSS and ITO are 154 and 164 cm^2/C, respectively. The comparable CE for the PEDOT on our composite film suggests that the composite can transfer charge uniformly. Moreover, it dose not consume additional injected or ejected charge, leading to a lower CE. The durability of the composite in aqueous media was also evaluated by measuring the electrochromic stability. Figure 8d demonstrates the transmittance attenuation for the PEDOT on the conductive composites as a function of cycling number between 1.0 and −1.0 V. After 200 double switches in the electrolyte, we observed an attenuation of transmittance of only 3%. These results indicate the Au-MWCNT after the plasma treatment can form a strongly mechanical conductive network within PEDOT:PSS. This can effectively reduce the charge transfer barrier and enhance the adhesion with the substrate and solvent resistance.

4. CONCLUSION

A novel hybrid transparent conductive material composed of Au-decorated MWCNT and PEDOT:PSS has been successfully synthesized. The Au NPs grown on the MWCNT can be covered with larger NPs via MW plasma irradiation. The sintered Au NPs connect the MWCNT within PEDOT:PSS forming a three-dimensional network to reduce the contact resistance. As a result, the Au-MWCNT/PEDOT:PSS composites exhibit a low sheet resistance of 51 Ω/sq with a high transparency of 86.2% at 550 nm. The composites are readily employed as transparent electrodes in flexible solar cells exhibiting competitive PCE with those of the ITO-based devices. In addition, the composite films are also integrated into the electrochromic devices showing high performance and durability in aqueous media. These properties make it well-suited for use as a conductive platform for next-generation flexible electronics.

AUTHOR INFORMATION

Corresponding Authors

*Address: 100 Shih-Chuan 1st Road, Kaohsiung 80708, Taiwan. E-mail: kclee@kmu.edu.tw. Telephone: +886-7-3121101, ext. 2818.

*Address: No. 2 Zuonan Rd., Nanzi District, Kaohsiung City 81126, Taiwan. E-mail: 295604@cpc.com.tw. Telephone: +886-7-5824141, ext. 7331.

Notes

The authors declare no competing financial interest.

ACKNOWLEDGMENTS

We are grateful to Kaohsiung Medical University (KMU) (KMU-Q104004) for financial support. We also are thankful for the research fundings from Taipei Medical University and the Ministry of Science and Technology (TMUTOP103004-2 and MOST103-2320-B-038-006-MY2).

REFERENCES

(1) Mativenga, M.; Geng, D.; Kim, B.; Jang, J. Fully Transparent and Rollable Electronics. *ACS Appl. Mater. Interfaces* **2015**, 7, 1578−1585.

DOI: 10.1021/acsami.5b03159
ACS Appl. Mater. Interfaces 2015, 7, 11668−11676

(2) Kim, J. Y.; Jeon, J. H.; Kwon, M. Indium Tin Oxide-Free Transparent Conductive Electrode for GaN-Based Ultraviolet Light-Emitting Diodes. *ACS Appl. Mater. Interfaces* **2015**, *7*, 7945−7950.
(3) Yuksel, R.; Sarioba, Z.; Cirpan, A.; Hiralal, P.; Unalan, H. E. Transparent and Flexible Supercapacitors with Single Walled Carbon Nanotube Thin Film Electrodes. *ACS Appl. Mater. Interfaces* **2014**, *6*, 15434−15439.
(4) Azzopardi, B.; Emmott, C. J. M.; Urbina, A.; Krebs, F. C.; Mutale, J.; Nelson, J. Economic Assessment of Solar Electricity Production from Organic-Based Photovoltaic moMules in a Domestic Environment. *Energy Environ. Sci.* **2011**, *4*, 3741−3753.
(5) Eggenhuisen, T. M.; Galagan, Y.; Coenen, E. W. C.; Voorthuijzen, W. P.; Slaats, M. W. L.; Kommeren, S. A.; Shanmuganam, S.; Coenen, M. J. J.; Andriessen, R.; Groen, W. A. Digital Fabrication of Organic Solar Cells by Inkjet Printing Using Non-Halogenated Solvents. *Sol. Energy Mater. Sol. Cells* **2014**, *4*, 5462−5469.
(6) Mengistie, D. A.; Wang, P. C.; Chu, C. W. Effect of Molecular Weight of Additives on the Conductivity of PEDOT:PSS and Efficiency for ITO-Free Organic Solar Cells. *J. Mater. Chem. A* **2013**, *1*, 9907−9915.
(7) Mukherjee, S.; Singh, R.; Gopinathan, S.; Murugan, S.; Gawali, S.; Saha, B.; Biswas, J.; Lodha, S.; Kumar, A. Solution-Processed Poly(3,4-ethylenedioxythiophene) Thin Films as Transparent Conductors: Effect of P-toluenesulfonic Acid in Dimethyl Sulfoxide. *ACS Appl. Mater. Interfaces* **2014**, *6*, 17792−17803.
(8) Galagan, Y.; Shanmugam, S.; Teunissen, J. P.; Eggenhuisen, T. M.; Biezemans, A. F. K. V.; Van Gijseghem, T.; Groen, W. A.; Andriessen, R. Solution Processing of Back Electrodes for Organic Solar Cells with Inverted Architecture. *Sol. Energy Mater. Sol. Cells* **2014**, *2*, 3175−3181.
(9) Kim, J. Y.; Jung, J. H.; Lee, D. E.; Joo, J. Enhancement of Electrical Conductivity of Poly(3,4-ethylenedioxythiophene)/Poly(4-styrenesulfonate) by a Change of Solvents. *Synth. Met.* **2002**, *126*, 311−316.
(10) Huang, J. H.; Kekuda, D.; Chu, C. W.; Ho, K. C. Electrochemical Characterization of the Solvent-Enhanced Conductivity of Poly(3,4-ethylenedioxythiophene) and Its Application in Polymer Solar Cells. *J. Mater. Chem.* **2009**, *19*, 3704−3712.
(11) Park, S.; Tark, S. J.; Kim, D. Effect of Sorbitol Doping in PEDOT:PSS on the Electrical Performance of Organic Photovoltaic Devices. *Curr. Appl. Phys.* **2011**, *6*, 1299−1301.
(12) Wang, T.; Qi, Y.; Xu, J.; Hu, X.; Chen, P. Effects of Poly(ethylene glycol) on Electrical Conductivity of Poly(3,4-ethylenedioxythiophene)−Poly(styrenesulfonic acid) Film. *Appl. Surf. Sci.* **2005**, *250*, 188−194.
(13) Ouyang, J.; Xu, Q.; Chu, C. W.; Yang, Y.; Li, G.; Shinar, J. On the Mechanism of Conductivity Enhancement in Poly(3,4-ethylenedioxythiophene):Poly(styrene sulfonate)Film through Solvent Treatment. *Polymer* **2004**, *45*, 8443−8450.
(14) Okuzaki, H.; Harashina, Y.; Yan, H. Highly Conductive PEDOT/PSS Microfibers Fabricated by Wet-Spinning and Dip-Treatment in Ethylene Glycol. *Eur. Polym. J.* **2009**, *1*, 256−261.
(15) Crispin, X.; Jakobsson, F. L. E.; Crispin, A.; Grim, P. C. M.; Andersson, P.; Volodin, A.; van Haesendonck, C.; Van der Auweraer, M.; Salaneck, W. R.; Berggren, M. The Origin of the High Conductivity of Poly(3,4-ethylenedioxythiophene)−Poly(styrenesulfonate) (PEDOT−PSS) Plastic Electrodes. *Chem. Mater.* **2006**, *18*, 4354−4360.
(16) Kim, Y. H.; Sachse, C.; Machala, M. L.; May, C.; Müller-Meskamp, L.; Leo, K. Highly Conductive PEDOT:PSS Electrode with Optimized Solvent and Thermal Post-Treatment for ITO-Free Organic Solar Cells. *Adv. Funct. Mater.* **2001**, *6*, 1076−1081.
(17) Xia, Y.; Ouyang, J. PEDOT:PSS Films with Significantly Enhanced Conductivities Induced by Preferential Solvation with Cosolvents and Their Application in Polymer Photovoltaic Cells. *J. Mater. Chem.* **2011**, *21*, 4927−4936.
(18) Fan, B.; Mei, X.; Ouyang, J. Significant Conductivity Enhancement of Conductive Poly(3,4-ethylenedioxythiophene):Poly(styrenesulfonate) Films by Adding Anionic Surfactants into Polymer Solution. *Macromolecules* **2008**, *41*, 5971−5973.
(19) Badre, C.; Marquant, L.; Alsayed, A. M.; Hough, L. A. Highly Conductive Poly(3,4-ethylenedioxythiophene):Poly(styrenesulfonate) Films Using 1-ethyl-3-methylimidazolium Tetracyanoborate Ionic Liquid. *Adv. Funct. Mater.* **2012**, *22*, 2723−2727.
(20) Ouyang, J. Solution-Processed PEDOT:PSS Films with Conductivities as Indium Tin Oxide through a Treatment with Mild and Weak Organic Acids. *ACS Appl. Mater. Interfaces* **2013**, *5*, 13082−13088.
(21) Mengistie, D. A.; Ibrahem, M. A.; Wang, P. C.; Chu, C. W. Highly Conductive PEDOT:PSS Treated with Formic Acid for ITO-Free Polymer Solar Cells. *ACS Appl. Mater. Interfaces* **2014**, *6*, 2292−2299.
(22) Xia, Y.; Sun, K.; Ouyang, J. Solution-Processed Metallic Conducting Polymer Films as Transparent Electrode of Optoelectronic Devices. *Adv. Mater. (Weinheim, Ger.)* **2012**, *24*, 2436−2440.
(23) Park, H. S.; Choi, B. G.; Hong, W. H.; Jang, S. Y. Interfacial Interactions of Single-Walled Carbon Nanotube/Conjugated Block Copolymer Hybrids for Flexible Transparent Conductive Films. *J. Phys. Chem. C* **2012**, *116*, 7962−7967.
(24) Allen, R.; Pan, L. J.; Fuller, G. G.; Bao, Z. A. Using In-Situ Polymerization of Conductive Polymers to Enhance the Electrical Properties of Solution-Processed Carbon Nanotube Films and Fibers. *ACS Appl. Mater. Interfaces* **2014**, *6*, 9966−9974.
(25) Alshammari, A. S.; Shkunov, M. Correlation between Wetting Properties and Electrical Performance of Solution Processed PEDOT:PSS/CNT Nano-Composite Thin Films. *Colloid Polym. Sci.* **2014**, *292*, 661−668.
(26) Li, G.; Shrotriya, V.; Huang, J.; Yao, Y.; Moriarty, T.; Emery, K.; Yang, Y. High-Efficiency Solution Processable Polymer Photovoltaic Cells by Self-Organization of Polymer Blends. *Nat. Mater.* **2005**, *4*, 864−868.
(27) Huang, J. H.; Fang, J. H.; Liu, C. C.; Chu, C. W. Effective Work Function Modulation of Graphene/Carbon Nanotube Composite Films as Transparent Cathodes for Organic Optoelectronics. *ACS Nano* **2011**, *5*, 6262−6271.
(28) Tummala, N. R.; Striolo, A. SDS Surfactants on Carbon Nanotubes: Aggregate Morphology. *ACS Nano* **2009**, *3*, 595−602.
(29) Wang, H.; Zhou, W.; Ho, D. L.; Winey, K. I.; Fischer, J. E.; Glinka, C. J.; Hobbie, E. K. Dispersing Single-Walled Carbon Nanotubes with Surfactants: Small Angle Neutron Scattering Study. *Nano Lett.* **2004**, *4*, 1789−1793.
(30) Moore, V. C.; Strano, M. S.; Haroz, E. H.; Hauge, R. H.; Smalley, R. E. Individually Suspended Single-Walled Carbon Nanotubes in Various Surfactants. *Nano Lett.* **2003**, *3*, 1379−1382.
(31) Grossiord, N.; Loos, J.; Regev, O.; Koning, C. E. Toolbox for Dispersing Carbon Nanotubes into Polymers to Get Conductive Nanocomposites. *Chem. Mater.* **2006**, *18*, 1089−1099.
(32) Grunlan, J. C.; Liu, L.; Regev, O. Weak Polyelectrolyte Control of Carbon Nanotube Dispersion in Water. *J. Colloid Interface Sci.* **2008**, *317*, 346−349.
(33) Dror, Y.; Pyckhout-Hintzen, W.; Cohen, Y. Conformation of Polymers Dispersing Single-Walled Carbon Nanotubes in Water: A Small-Angle Neutron Scattering Study. *Macromolecules* **2005**, *38*, 7828−7836.
(34) Haggenmueller, R.; Rahatekar, S. S.; Fagan, J. A.; Chun, J.; Becker, M. L.; Naik, R. R.; Krauss, T.; Carlson, L.; Kadla, J. F.; Trulove, P. C.; Fox, D. F.; Delong, H. C.; Fang, Z.; Kelley, S. O.; Gilman, J. W. Comparison of the Quality of Aqueous Dispersions of Single Wall Carbon Nanotubes Using Surfactants and Biomolecules. *Langmuir* **2008**, *24*, 5070−5078.
(35) Zheng, M.; Jagota, A.; Semke, E. D.; Diner, B. A.; Mclean, R. S.; Lustig, S. R.; Richardson, R. E.; Tassi, N. G. DNA-Assisted Dispersion and Separation of Carbon Nanotube. *Nat. Mater.* **2003**, *2*, 338−342.
(36) Kim, D.; Kim, Y.; Choi, K.; Grunlan, J. C.; Yu, C. Improved Thermoelectric Behavior of Nanotube-Filled Polymer Composites with Poly(3,4-ethylenedioxythiophene):Poly(styrenesulfonate). *ACS Nano* **2010**, *4*, 513−523.

DOI: 10.1021/acsami.5b03159
ACS Appl. Mater. Interfaces 2015, 7, 11668−11676

(37) Hermant, M. C.; Klumperman, B.; Kyrylyuk, A. V.; van der Schoot, P.; Koning, C. E. Lowering the Percolation Threshold of Single-Walled Carbon Nanotubes Using Polystyrene/Poly(3,4-ethylenedioxythiophene):Poly(styrene sulfonate) Blends. *Soft Matter* **2009**, *5*, 878−885.
(38) Jalili, R.; Razal, J. M.; Wallance, G. G. Exploiting High Quality PEDOT:PSS−SWNT Composite Formulations for Wet-Spinning Multifunctional Fibers. *J. Mater. Chem.* **2012**, *22*, 25174−25182.
(39) Sun, Z.; Nicolosi, V.; Rickard, D.; Bergin, S. D.; Aherne, D.; Coleman, J. N. Quantitative Evaluation of Surfactant-Stabilized Single-Walled Carbon Nanotubes: Dispersion Quality and Its Correlation with ζ Potential. *J. Phys. Chem. C* **2008**, *112*, 10692−10699.
(40) O'Connell, M. J.; Boul, P.; Ericson, L. M.; Hufffman, C.; Wang, Y.; Haroz, E.; Kuper, C.; Tour, J. M.; Ausman, K. D.; Smalley, R. E. Reversible Water-Solubilization of Single-Walled Carbon Nanotubes by Polymer Wrapping. *Chem. Phys. Lett.* **2001**, *342*, 265−271.
(41) Ingle, J. D. J.; Crouch, S. R. *Spectrochemical Analysis*; Prentice Hall: Englewood Cliffs, NJ, 1988; p 372.

DOI: 10.1021/acsami.5b03159
ACS Appl. Mater. Interfaces 2015, 7, 11668−11676